

Communication

# Halogen-Substituted Triazolethioacetamides as a Potent Skeleton for the Development of Metallo- $\beta$ -Lactamase Inhibitors

Yilin Zhang <sup>1,\*</sup>, Yong Yan <sup>1</sup>, Lufan Liang <sup>1</sup>, Jiefeng <sup>1</sup>, Xuejun Wang <sup>1</sup>, Li Li <sup>1</sup> and Kewu Yang <sup>2</sup>

<sup>1</sup> College of Biology Pharmacy and Food Engineering, Shangluo University, Shangluo 726000, China; yananan@yeah.net (Y.Y.); lianglouyv@163.com (L.L.); jiefeng\_ab123@163.com (J.F.); xuejunwangd@163.com (X.W.); Lily8028@163.com (L.L.)

<sup>2</sup> Key Laboratory of Synthetic and Natural Functional Molecule Chemistry of Ministry of Education, College of Chemistry and Materials Science, Northwest University, Xi'an 710127, China; kwyang@nwu.edu.cn

\* Correspondence: 233049@slxy.edu.cn; Tel.: +86-15091567430

Received: 1 January 2019; Accepted: 23 March 2019; Published: 25 March 2019



**Abstract:** Metallo- $\beta$ -lactamases (M $\beta$ Ls) are the target enzymes of  $\beta$ -lactam antibiotic resistance, and there are no effective inhibitors against M $\beta$ Ls available for clinic so far. In this study, thirteen halogen-substituted triazolethioacetamides were designed and synthesized as a potent skeleton of M $\beta$ Ls inhibitors. All the compounds displayed inhibitory activity against ImiS with an IC<sub>50</sub> value range of 0.032–15.64  $\mu$ M except 7. The chlorine substituted compounds (**1**, **2** and **3**) inhibited NDM-1 with an IC<sub>50</sub> value of less than 0.96  $\mu$ M, and the fluorine substituted **12** and **13** inhibited VIM-2 with IC<sub>50</sub> values of 38.9 and 2.8  $\mu$ M, respectively. However, none of the triazolethioacetamides exhibited activity against L1 at inhibitor concentrations of up to 1 mM. Enzyme inhibition kinetics revealed that **9** and **13** are mixed inhibitors for ImiS with K<sub>i</sub> values of 0.074 and 0.27  $\mu$ M using imipenem as the substrate. Docking studies showed that **1** and **9**, which have the highest inhibitory activity against ImiS, fit the binding site of CphA as a replacement of ImiS via stable interactions between the triazole group bridging ASP120 and hydroxyl group bridging ASN233.

**Keywords:** halogen-substituted triazolethioacetamides; M $\beta$ Ls; inhibitor

## 1. Introduction

$\beta$ -Lactam antibiotics containing a four membered  $\beta$ -lactam ring are a major class of antibiotics, accounting for over 65% of injectable antibiotics in clinic [1]. However, antibacterial resistance caused by the overuse of antibiotics has become a threat to global public health. The main mechanisms of resistance to  $\beta$ -lactam antibiotics is the expression of  $\beta$ -lactamase from bacteria, which can catalyze the hydrolysis of the C-N bond of the  $\beta$ -lactam ring to deactivate the antibiotics [2,3]. So far, there have been more than 2000 distinct  $\beta$ -lactamases identified [4]. Based on amino acid sequence homology,  $\beta$ -lactamases can be divided into four classes: Classes A, C and D, known as serine- $\beta$ -lactamases (SBLs), can restore the efficacy of  $\beta$ -lactam antibiotics by a successful clinic combination drug therapy with SBL inhibitors (sulbactam, tazobactam and clavulanic acid) [5,6]; Class B enzymes, known as metallo- $\beta$ -lactamases (M $\beta$ Ls), display activity by one or two Zn ions in the active sites, which are further divided into subclasses B1-B3 [6,7]. Although a number of promising inhibitor molecules have been reported in recent years, there are no effective inhibitors against M $\beta$ Ls available for clinical therapy [8]. More seriously, new Delphi metallo- $\beta$ -lactamase 1 (NDM-1), which were first identified from pathogenic bacterium in 2008 and classified as B1 subclass M $\beta$ Ls, greatly aggravates the challenge to treat bacterial infection in clinic because of the ability to hydrolyze almost all  $\beta$ -lactam

antibiotics [9–11]. Obviously, lack of knowledge about catalytic mechanisms of NDM-1 has delayed the development of clinical inhibitors [12].

In 2016, Mojica et al. reported that the pace of the development of M $\beta$ LS inhibitors has slowed, which was mainly because a shallow, relatively featureless active site and few scaffolds that can selectively attach to the active site [13]. Mollard et al. reported that thiomandelic acid was capable of potential broad spectrum M $\beta$ LS inhibitors with  $K_i$  values of 0.09  $\mu$ M for rthiomandelic acid and 1.28  $\mu$ M for the S-isomer. Moreover, the thiol group can bind the two zinc ions which is the active site of M $\beta$ LS [14]. The Weide et al. research group developed more than 200 sulfotriazole derivatives, and there were 31 compounds which had inhibitory activity against VIM-2 with  $K_i$  values ranging from 0.01–0.39  $\mu$ M [15]. The N-methyl mercaptosulfonylhydrazole compounds substituted containing trifluoromethyl could inhibit M $\beta$ LS in competing mode, the enzyme activity test showed that the mercapto group was the necessary group to produce the activity [16].

In our group's preliminary work, we found that the azolythioacetamides scaffold has potential inhibition for M $\beta$ LS, and the aryl-substituted thioacetamides containing the triazole group can effectively inhibit ImiS and NDM-1 [17–20]. In addition, four of the azolythioacetamides exhibit broad-spectrum inhibitory activity against all three subclasses of M $\beta$ LS [17]. Based on the research, we want to develop new azolythioacetamides by conjugation of the triazole and thioacetamides company with halogen to find effective M $\beta$ LS inhibitors. To further explore the structure-activity relationships of the azolythioacetamide compounds, thirteen halogen-substituted triazolethioacetamides were synthesized and eleven of that were novel compounds. Their potential as M $\beta$ LS inhibitors were evaluated with the enzymes VIM-2, NDM-1, ImiS and L1, which are representatives of the B1, B2 and B3 subclasses of M $\beta$ LS. Also, molecule docking was adopted to explore the binding method between inhibitors and M $\beta$ LS.

## 2. Results and Discussion

The thirteen halogen-substituted triazolethioacetamides were designed and synthesized as listed in Figure 1 and the synthetic procedures were available in Scheme 1. Briefly, the crosslink between 2-(5-mercapto-4H-1,2,4-triazol-3-yl) phenol (s4) and R-substituted-2-chloro-N-phenyl -acetamide (N1-13) gave the corresponding target compounds (1–13). All compounds were characterized by  $^1$ H and  $^{13}$ C NMR and confirmed by MS.

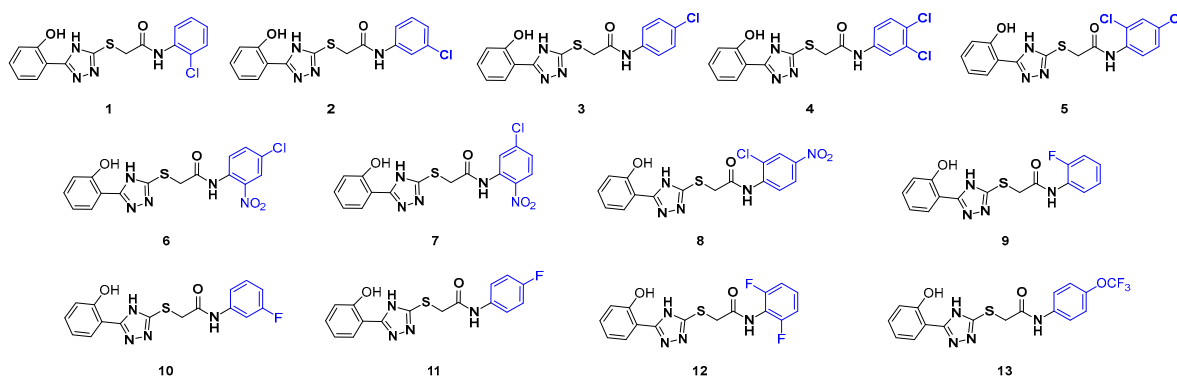


Figure 1. The halogen-substituted triazolethioacetamides.



**Table 1.** IC<sub>50</sub> values of azolylthioacetamides against MβLs (μM).

Compds	ImiS	NDM-1	VIM-2
1	0.032 ± 0.004	0.96 ± 0.07	- <sup>1</sup>
2	0.045 ± 0.002	0.17 ± 0.02	-
3	0.051 ± 0.006	0.37 ± 0.05	-
4	0.27 ± 0.02	-	-
5	0.16 ± 0.03	-	-
6	0.78 ± 0.08	-	-
7	0.20 ± 0.04	-	-
8	0.26 ± 0.03	-	-
9	0.072 ± 0.005	-	-
10	0.98 ± 0.04	-	-
11	>50	-	-
12	15.64 ± 3	-	38.9 ± 5
13	0.23 ± 0.09	-	2.8 ± 0.3

<sup>1</sup>—: no inhibition at an inhibitor concentration of 1 mM.

To identify the inhibition mode of the halogen-substituted azolylthioacetamides against MβLs, typical representatives **9** and **13** for ImiS were chosen to determine  $K_i$  values. Lineweaver–Burk plots of ImiS catalyzed hydrolysis of imipenem in the absence and presence of inhibitors are displayed in Figure 2. Compounds **9** and **13** exhibited  $K_i$  values of 0.074 and 0.27 μM, respectively, which are slightly larger than their correlative IC<sub>50</sub> values. The analysis also demonstrated that all the compounds employed the same partially mixed inhibition type.

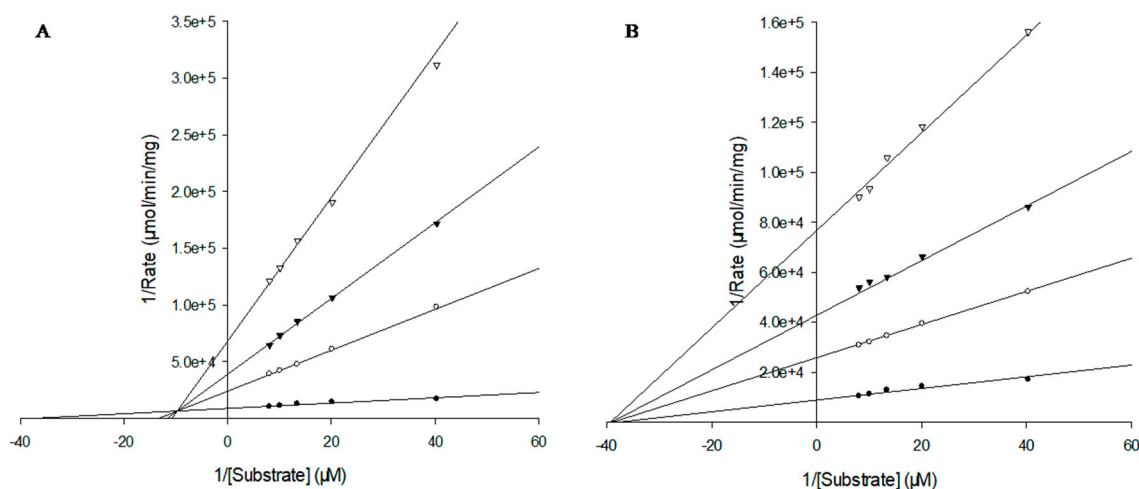


**Figure 2.** Lineweaver–Burk plot of ImiS catalyzed hydrolysis of imipenem in the absence and presence of **9** (A) and **13** (B). Inhibitor concentrations were 0 μM (●), 0.25 μM (○), 0.5 μM (▼), and 1.0 μM (▽).

Molecular docking analysis was achieved from three comparable conformations (out of 50) docked into corresponding target protein for four representative halogen-substituted triazolethioacetamides. Because there is no high-resolution crystal structure of ImiS available, the very closely related (96% sequence identity) CphA was used instead. The lowest-energy conformations were shown in Figure 3, with the binding energies of  $-7.6$ ,  $-7.47$ ,  $-7.75$ ,  $-6.99$  and  $-5.87$  kcal/mol for the CphA/**1**, CphA/**9**, CphA/**13**, NDM-1/**2** and VIM-2/**13** complexes, respectively.

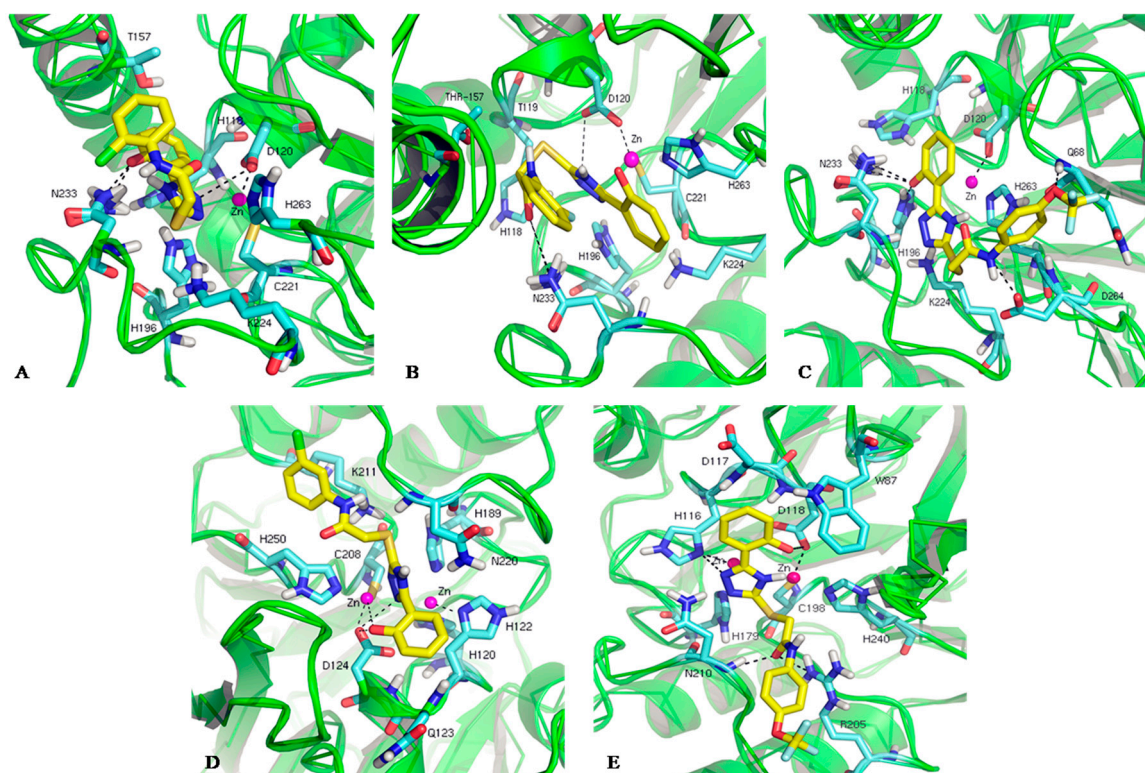


**Figure 3.** Low energy conformations of **1**, **9** and **13** docked into the active site of CphA (PDB code 2QDS) (A–C), **2** docked into NDM-1 (PDB code 4EYL) (D) and **13** docked into VIM-2 (PDB code 4NQ2) (E). The enzyme backbone is shown as cartoon in green, and the Zn(II) ions are shown as magenta spheres. Colored sticks by element were used to show ligand (C, yellow; N, blue; O, red; S, sand; Cl, viridis; F: cyan; H, grey) and the residue side chains (C, cyan; N, blue; O, red; S, yellow; H, grey). The interactions between the inhibitors and enzyme residues were displayed by dashed lines.

Docking studies reveal that **1** and **9**, which exhibited the lowest  $IC_{50}$  values with ImiS, have similar binding patterns with residue side chains in CphA (Figure 3A,B). The triazole group both interact with ASP120 at distances of less than  $3.48 \text{ \AA}$ , and hydroxyl group of **1** and **9** interact with ASN233 at average distances of  $2.11$  and  $3.25 \text{ \AA}$ , which may result a  $0.13 \text{ kcal/mol}$  more favorable binding energy relative to **9**. Compound **13** with trifluoromethoxy group did not bind ASP120 together with Zn(II) ions as **1** and **9** did, but via three different interaction modes to get the lowest bonding energy for CphA with distances between  $1.89$  and  $3.21 \text{ \AA}$ , the interactions are the amide carbonyl group and ASP264, the trifluoromethoxy group and GLN68, the hydroxyl group interact with ASN233 and H196. This may explain why although the docking binding energy of CphA/**1** ( $-7.6 \text{ kcal/mol}$ ) and CphA/**9** ( $-7.47 \text{ kcal/mol}$ ) complexes are larger than CphA/**13** ( $-7.75 \text{ kcal/mol}$ ), **1** and **9** showed more inhibitory potency against CphA. However, the docking mode of VIM-2/**13** complex continued to change, one is the amide carbonyl group form hydrogen bonds with ASN210 and ARG 205, the other is that the interaction between the triazole group and H116, and, in addition, the hydroxyl group that interacts with ASP118. In compound **2**, the hydroxyl group coordinates at Zn(II) ions of NDM-1 in comparable distances of  $3.59 \text{ \AA}$ , the hydroxyl group and triazole group both interact with ASP 124. The docking results reveal that the triazole ring of these compounds plays an important role in the interactions with the close residue side chains, meanwhile there is rarely any direct interaction with active site Zn(II) ions as seen in previous findings, which may be due to the introduction of halogen, nitro and trifluoromethoxy influence the relectrostatic interactions between ligand and target protein.

It was interesting to observe that the compounds had different activity against VIM-2 and NDM-1, even though the active sites of NDM-1 and VIM-2 are quite similar. There are two differences between the enzymes which may be significant for the inhibitor binding  $M\beta$ LS: (1) The distance between Zn(II)

ion and Asp124 which interacts with the hydroxyl group and the triazole ring of **2** in NDM-1, is bigger in VIM-2 (16.12 Å, PDB code 4NQ2) than in NDM-1 (2.12 Å, PDB code 4EYL). Thus it is impossible to establish effective interaction among the hydroxyl group, Asp124 and Zn(II) ion in VIM-2. (2) VIM-2 has a histidine at position 116 and an aspartic acid at position 118, which are the co-interacting amino acids of active center Zn(II) ion and **13**. However, NDM-1 has a histidine and valine at the same corresponding position, so **13** is difficult to show activity against NDM-1.

Methyl group is the isosteric surrogate of chlorine. If the chlorine of compound **1** was replaced by methyl group, the methyl substituted triazolethioacetamides only inhibit NDM-1 with an IC<sub>50</sub> value of 0.16 µM [18], which is significantly higher than that of compound **1**, but no inhibitory activity was observed against ImiS. From Figure 3, it is obvious to observe that the triazolethioacetamides are embedded in the active pocket of ImiS in folding mode, and binded to the NDM-1 active center in a relatively stretched state. The methyl group will increase steric hindrance of inhibitor molecules, and weaken the ability to combine ImiS. Thus, hindrance of substituents can not only change the conformation of triazolethioacetamides, but also affect the interaction between triazolethioacetamides and MβLs.

### 3. Materials and Methods

#### 3.1. General Information

General chemicals were purchased from TCI (Tokyo Chemical Industry, Tokyo, Japan) and were used without further purification. All antibiotics used were purchased from Sigma-Aldrich (St. Louis, MO, USA). <sup>1</sup>H NMR and <sup>13</sup>C NMR spectra were recorded on a NMR spectra were recorded with a Bruker DRX 600 MHz spectrometer (Bruker Daltonics Inc., Billerica, MA, USA). The peaks patterns are indicated as follows: s, singlet; d, doublet; t, triplet; q, quartet; dd, doublet doublet; m, multiplet. The spectra were recorded with TMS as internal standard. Coupling constants (J) were reported in hertz (Hz). Chemical shifts were given in part per million (ppm) on the delta scale. Analytical Thin Layer Chromatography (TLC) was carried out on silica gel F<sub>254</sub> plates with visualization by ultraviolet radiation. HRMS spectra were recorded on a Bruker MicrOTOF-Q II (Bruker Daltonics Inc., Billerica, MA, USA) mass spectrometer. Inhibition studies were performed on an Agilent-8453 UV-visible spectrometer (Santa Clara, CA, USA).

#### 3.2. Synthesis and Characterization

Briefly, R-substituted-2-chloro-N-phenylacetamide (**N1–13**) and the intermediate 2-(5-mercapto-4H-1,2,4-triazol-3-yl)phenol (**s4**) were prepared as previously reported [17]. A solution of 2-(5-mercapto-4H-1,2,4-triazol-3-yl) phenol (**s4**) (3 mmol) and NaOH (3.6 mmol) dissolved in H<sub>2</sub>O (15 mL) was added in a 50 mL three-neck round bottomed flask, kept stirring for 30 min. N-substituted-2-chloroacetamides (**N1–13**) (3 mmol) in hot ethanol (5 mL) was added drop wise to the mix solution, and the slurry was stirred at reflux for 6 h. The resulting solution was cooled and neutralized with HCl (5M) to pH 7.0. The resulting white precipitate (**1–13**) was filtered off, washed with water (3 × 80 mL), and dried in vacuo. The spectrogram information for the target compounds was shown in the Supplementary Data.

#### 3.3. Determination of IC<sub>50</sub> and K<sub>i</sub> values

The inhibition studies were carried out on an Agilent UV 8453 spectrophotometer at 25 °C using cefazolin as substrate of CcrA, NDM-1, and L1 and imipenem as substrate of ImiS. Inhibitors **1–13** were dissolved in DMSO and then diluted with Tris-HCl, pH 7.0. The substrate concentrations were varied between 25 and 400 µM, and inhibitor concentrations were varied between 125 nM and 1 mM. The enzyme and inhibitor were pre-incubated for 30 min before starting the kinetic experiments. The IC<sub>50</sub> values for all analyzed compounds were calculated based on the kinetic data. The mode

of inhibition was determined by generating Lineweaver-Burk plots of the data [23], and the  $K_i$  was determined by replotting the data for slope and intercept versus substrate concentration.

### 3.4. Docking Calculations

Inhibitors were docked into the active sites of NDM-1 (PDB code 4EYL), CphA (PDB code 2QDS), VIM-2 (PDB code 4NQ2). The program AutoDock 4.2 [25] was used for molecule docking analysis. The flexible ligand was docked into each rigid monomeric receptor using a grid box with equal space of 0.375 Å per grid and center of the one or two active-site Zn(II) ions. Fifty conformations were generated for each complex. The rest of the parameters were set at their default values and all docking calculations were performed without constraints. Binding energies were calculated via the Lamarckian genetic algorithm and conformations that constitute each cluster were defined by a root mean square deviation tolerance.

## 4. Conclusions

In summary, we have successfully developed a potent skeleton as MβLs inhibitors, and thirteen halogen-substituted triazolethioacetamides were synthesized and characterized by NMR and MS. Biological activity assays reveal that the triazolethioacetamides have special potency to inhibit ImiS with the lowest IC<sub>50</sub> value of 32 nM, and compound 1–3 with chlorine group display mix inhibition against NDM-1 with a IC<sub>50</sub> range from 170 to 960 nM. Meanwhile, 12 with two fluorine group and 13 with trifluoromethoxy group show certain inhibitory activity against VIM-2 in vitro. Docking studies reveal that the triazolethioacetamides, which can form stable interactions with the triazole bridging ASP120, and the phenolichydroxyl group interacting with ASN233 in CphA, promote the inhibitory activity against ImiS. The identification of thirteen halogen-substituted triazolethioacetamides which show that a mix mode of inhibition provides potent information for the further development of inhibitors against MβLs.

**Supplementary Materials:** The <sup>1</sup>H NMR, <sup>13</sup>C NMR and HRMS spectra data of all the target compounds were provided in supporting information.

**Author Contributions:** The manuscript was written through contributions of all authors. Y.Z. designed and conducted the experiments, analyzed the data, prepared the original draft and funding acquisition; Y.Y. provided synthesis and software support, reviewed and edited the draft; L.L. (Lufan Liang) and J.F. completed the synthesis assay and enzyme kinetic experiments; X.W. and L.L. (Li Li) conducted Docking assay; K.Y. provided the enzymes used in the experiment.

**Funding:** This work was supported by the Natural Science Foundation of Shaanxi Province (2018JQ2070), the Scientific Research Plan Project by Educational Department of Shaanxi Province (18JK0250), the Natural Science Foundation of Shangluo University (16SKY021) and the National Student's Innovation and Entrepreneurship Training Program (201711396005).

**Acknowledgments:** Thanks all the funds mentioned above for their support. Inhibition study was carried out in key laboratory of synthetic and natural functional molecule chemistry of ministry of education at Northwest University. All the enzymes used in the study were donated from Ke-wu Yang.

**Conflicts of Interest:** The authors declare no conflict of interest.

## References

1. Docquier, J.D.; Mangani, S. An update on β-lactamase inhibitor discovery and development. *Drug Resist. Updat.* **2018**, *36*, 13–29. [[CrossRef](#)] [[PubMed](#)]
2. Li, W.; Dong, K.; Ren, J.; Qu, X. A β-lactamase-imprinted responsive hydrogel for the treatment of antibiotic-resistant bacteria. *Angew. Chem. Int. Ed. Engl.* **2016**, *55*, 8049–8053. [[CrossRef](#)] [[PubMed](#)]
3. Rizk, N.A.; Kanafani, Z.A.; Tabaja, H.Z.; Kanj, S.S. Extended infusion of β-lactam antibiotics: Optimizing therapy in critically-ill patients in the era of antimicrobial resistance. *Expert Rev. Anti-Infect. Ther.* **2017**, *15*, 645–652. [[CrossRef](#)] [[PubMed](#)]
4. Bush, K. Past and present perspectives on β-lactamases. *Antimicrob. Agents Chemother.* **2018**, *62*, 01076–01118. [[CrossRef](#)] [[PubMed](#)]

5. Bush, K.; Bradford, P.A. Interplay between  $\beta$ -lactamases and new  $\beta$ -lactamase inhibitors. *Nat. Rev. Microbiol.* **2019**, *1*. [[CrossRef](#)] [[PubMed](#)]
6. Brem, J.; Cain, R.; Cahill, S.; McDonough, M.A.; Clifton, I.J.; Jimenez-Castellanos, J.C.; Avison, M.B.; Spencer, J.; Fishwick, C.W.; Schofield, C.J. Structural basis of metallo- $\beta$ -lactamase, serine- $\beta$ -lactamase and penicillin-binding protein inhibition by cyclic boronates. *Nat. Commun.* **2016**, *7*, 1–8. [[CrossRef](#)] [[PubMed](#)]
7. Crowder, M.W.; Spencer, J.; Vila, A.J. Metallo- $\beta$ -lactamases: Novel weaponry for antibiotic resistance in bacteria. *Acc. Chem. Res.* **2006**, *39*, 721–728. [[CrossRef](#)] [[PubMed](#)]
8. Ju, L.C.; Cheng, Z.; Fast, W.; Bonomo, R.A.; Crowder, M.W. The continuing challenge of metallo- $\beta$ -lactamase inhibition: Mechanism matters. *Trends Pharmacol. Sci.* **2018**, *39*, 635–647. [[CrossRef](#)] [[PubMed](#)]
9. Walsh, T.R.; Weeks, J.; Livermore, D.M.; Toleman, M.A. Dissemination of NDM-1 positive bacteria in the New Delhi environment and its implications for human health: An environmental point prevalence study. *Lancet Infect Dis.* **2011**, *11*, 355–362. [[CrossRef](#)]
10. Ali, A.; Gupta, D.; Srivastava, G.; Sharma, A.; Khan, A.U. Molecular and computational approaches to understand resistance of New Delhi metallo  $\beta$ -lactamase variants (NDM-1, NDM-4, NDM-5, NDM-6, NDM-7)-producing strains against carbapenems. *J. Biomol. Struct Dyn.* **2018**. [[CrossRef](#)] [[PubMed](#)]
11. Lu, Y.; Liu, W.; Liang, H.; Zhao, S.; Zhang, W.; Liu, J.; Jin, C.; Hu, H. NDM-1 encoded by a pNDM-HN380-like plasmid pNDM-BJ03 in clinical *Enterobacter cloacae*. *Diagn Microbiol. Infect Dis.* **2018**, *90*, 153–155.
12. Chen, J.; Wang, J.; Zhu, W. Zinc ion-induced conformational changes in new Delhi metallo-beta-lactamase 1 probed by molecular dynamics simulations and umbrella sampling. *Phys. Chem. Chem. Phys.* **2017**, *19*, 3067–3075. [[CrossRef](#)] [[PubMed](#)]
13. Mojica, M.F.; Bonomo, R.A.; Fast, W. B1-metallo- $\beta$ -lactamases: Where do we stand? *Curr. Drug Targets* **2016**, *17*, 1029–1050. [[CrossRef](#)]
14. Mollard, C.; Moali, C.; Papamicael, C.; Damblon, C.; Vessilier, S.; Amicosante, G.; Schofield, C.J.; Galleni, M.; Frere, J.M.; Roberts, G.C. Thiomandelic acid, a broad spectrum inhibitor of zinc  $\beta$ -lactamases: Kinetic and spectroscopic studies. *J. Biol. Chem.* **2001**, *276*, 45015–45023.
15. Weide, T.; Saldanha, S.A.; Minond, D.; Spicer, T.P.; Fotsing, J.R.; Spaargaren, M.; Frere, J.M.; Bebrone, C.; Sharpless, K.B.; Hodder, P.S.; et al. NH-1,2,3-Triazole-based inhibitors of the VIM-2 metallo- $\beta$ -lactamase: Synthesis and structure-activity studies. *ACS Med. Chem. Lett.* **2010**, *1*, 150–154. [[CrossRef](#)] [[PubMed](#)]
16. Vella, P.; Hussein, W.M.; Leung, E.W.; Clayton, D.; Ollis, D.L.; Mitic, N.; Schenk, G.; McGeary, R.P. The identification of new metallo- $\beta$ -lactamase inhibitor leads from fragment-based screening. *Bioorg. Med. Chem. Lett.* **2011**, *21*, 3282–3285. [[CrossRef](#)] [[PubMed](#)]
17. Zhang, Y.L.; Yang, K.W.; Zhou, Y.J.; LaCuran, A.E.; Oelschlaeger, P.; Crowder, M.W. Diaryl-substituted azolythioacetamides: Inhibitor discovery of New Delhi metallo- $\beta$ -lactamase-1 (NDM-1). *Chem. Med. Chem.* **2014**, *9*, 2445–2448. [[CrossRef](#)] [[PubMed](#)]
18. Zhai, L.; Zhang, Y.L.; Kang, J.S.; Oelschlaeger, P.; Xiao, L.; Nie, S.S.; Yang, K.W. Triazolylthioacetamide: A valid scaffold for the development of New Delhi metallo- $\beta$ -lactamase-1 (NDM-1) inhibitors. *ACS Med. Chem. Lett.* **2016**, *7*, 413–417. [[CrossRef](#)] [[PubMed](#)]
19. Xiang, Y.; Chang, Y.N.; Ge, Y.; Kang, J.S.; Zhang, Y.L.; Liu, X.L.; Oelschlaeger, P.; Yang, K.W. Azolythioacetamides as a potent scaffold for the development of metallo- $\beta$ -lactamase inhibitors. *Bioorg. Med. Chem. Lett.* **2017**, *27*, 5225–5229.
20. Shao-Kang, Y.; Kang, J.S.; Peter, O.; Ke-Wu, Y. Azolythioacetamide: A Highly Promising Scaffold for the Development of Metallo- $\beta$ -lactamase Inhibitors. *ACS Med. Chem. Lett.* **2015**, *6*, 455–460.
21. Yang, H.; Aitha, M.; Hetrick, A.M.; Richmond, T.K.; Tierney, D.L.; Crowder, M.W. Mechanistic and spectroscopic studies of metallo- $\beta$ -lactamase NDM-1. *Biochemistry* **2012**, *51*, 3839–3847. [[CrossRef](#)] [[PubMed](#)]
22. Crawford, P.A.; Sharma, N.; Chandrasekar, S.; Sigdel, T.; Walsh, T.R.; Spencer, J.; Crowder, M.W. Over-expression, purification, and characterization of metallo- $\beta$ -lactamase ImiS from *Aeromonas veronii* bv. *sobria*. *Protein Expr. Purif.* **2004**, *36*, 272–279. [[CrossRef](#)] [[PubMed](#)]
23. Crowder, M.W.; Walsh, T.R.; Banovic, L.; Pettit, M.; Spencer, J. Overexpression, purification, and characterization of the cloned metallo- $\beta$ -lactamase L1 from *Stenotrophomonas maltophilia*. *Antimicrob. Agents Chemother.* **1998**, *42*, 921–926. [[CrossRef](#)]



24. Moya, B.; Barcelo, I.M.; Bhagwat, S.; Patel, M.; Bou, G.; Papp-Wallace, K.M.; Bonomo, R.A.; Oliver, A. WCK 5107 (Zidebactam) and WCK 5153 Are Novel Inhibitors of PBP2 Showing Potent “ $\beta$ -lactam enhancer” activity against *Pseudomonas aeruginosa*, including multidrug-resistant metallo- $\beta$ -Lactamase-producing high-risk clones. *Antimicrob. Agents Chemother.* **2017**, *61*, 02529–02616. [[CrossRef](#)]
25. Forli, S.; Huey, R.; Pique, M.E.; Sanner, M.F.; Goodsell, D.S.; Olson, A.J. Computational protein-ligand docking and virtual drug screening with the AutoDock suite. *Nat. Protoc.* **2016**, *11*, 905–919. [[CrossRef](#)] [[PubMed](#)]

**Sample Availability:** All the target compounds halogen-substituted triazolethioacetamides are available from the authors, the synthetic raw materials are purchased from the reagent company and the metallo-beta-lactamase used in the manuscript were provided from Professor Ke-wu Yang.



© 2019 by the authors. Licensee MDPI, Basel, Switzerland. This article is an open access article distributed under the terms and conditions of the Creative Commons Attribution (CC BY) license (<http://creativecommons.org/licenses/by/4.0/>).